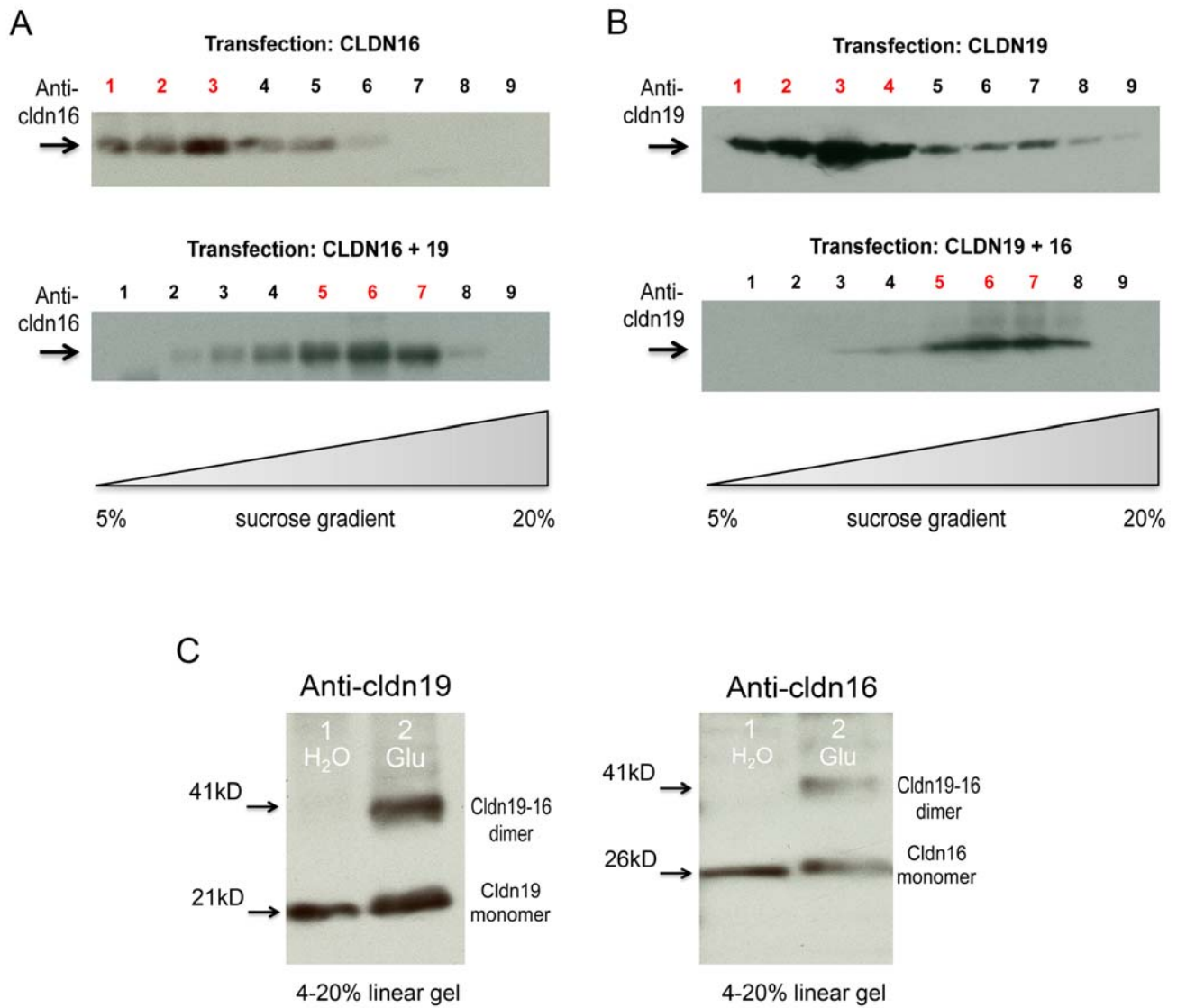


# Supplemental Materials

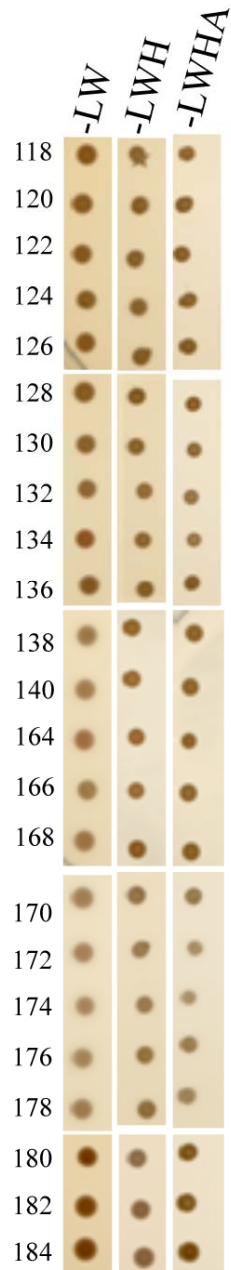
*Molecular Biology of the Cell*

Gong et al.



**Figure S1.** Biochemical analyses of claudin-16 and -19 assembly in Sf9 cells. Triton soluble cell lysate from singly or doubly infected claudin expressing cells were fractionated on 5-20% linear sucrose gradients and blotted with anti-claudin-16 (A) or anti-claudin-19 (B) antibody. (C) Linear SDS-PAGE gel electrophoresis to determine the molecular weight of claudin oligomer and monomer.

## Cldn19/pAlg5



## Cldn16/pAlg5

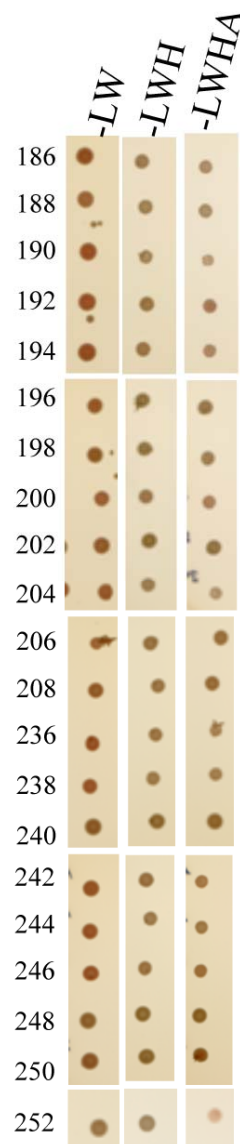


**Figure S2.** Determination of protein folding using Y2H. The claudin-16 or -19 mutant proteins were co-expressed with the yeast ER protein Alg5 in the bait-prey format. If the mutant claudin protein passes ER quality control and is properly inserted into the plasma membrane, co-expression with Alg5 will result in activation of reporter genes due to direct binding of Alg5 with ubiquitin that is fused to the mutant protein. Shown are plates with selective medium lacking leucine and tryptophan (–LW), indicating the transforming of both bait and prey vectors; with SD-LWH, indicating the expression of reporter gene HIS3; with SD-LWHA, indicating the expression of reporter genes HIS3 and ADE2.

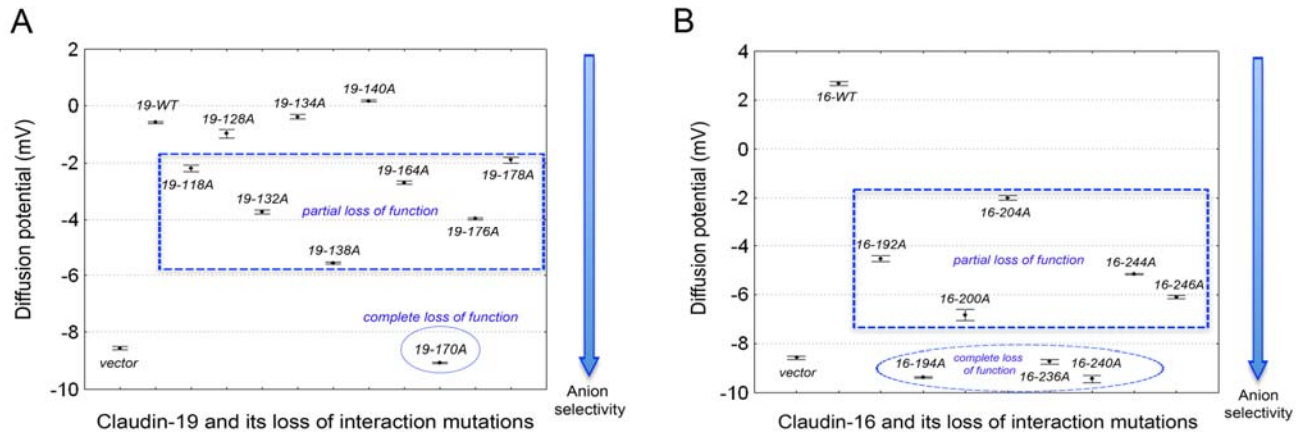


**Figure S3.** Effect of alanine insertion mutations on claudin function. (A) Diffusion potential values across LLC-PK1 cell monolayers expressing wildtype claudin-19 and its loss-of-interaction mutations are shown. (B) Diffusion potential values across LLC-PK1 cell monolayers expressing wildtype claudin-16 and its loss-of-interaction mutations are shown.

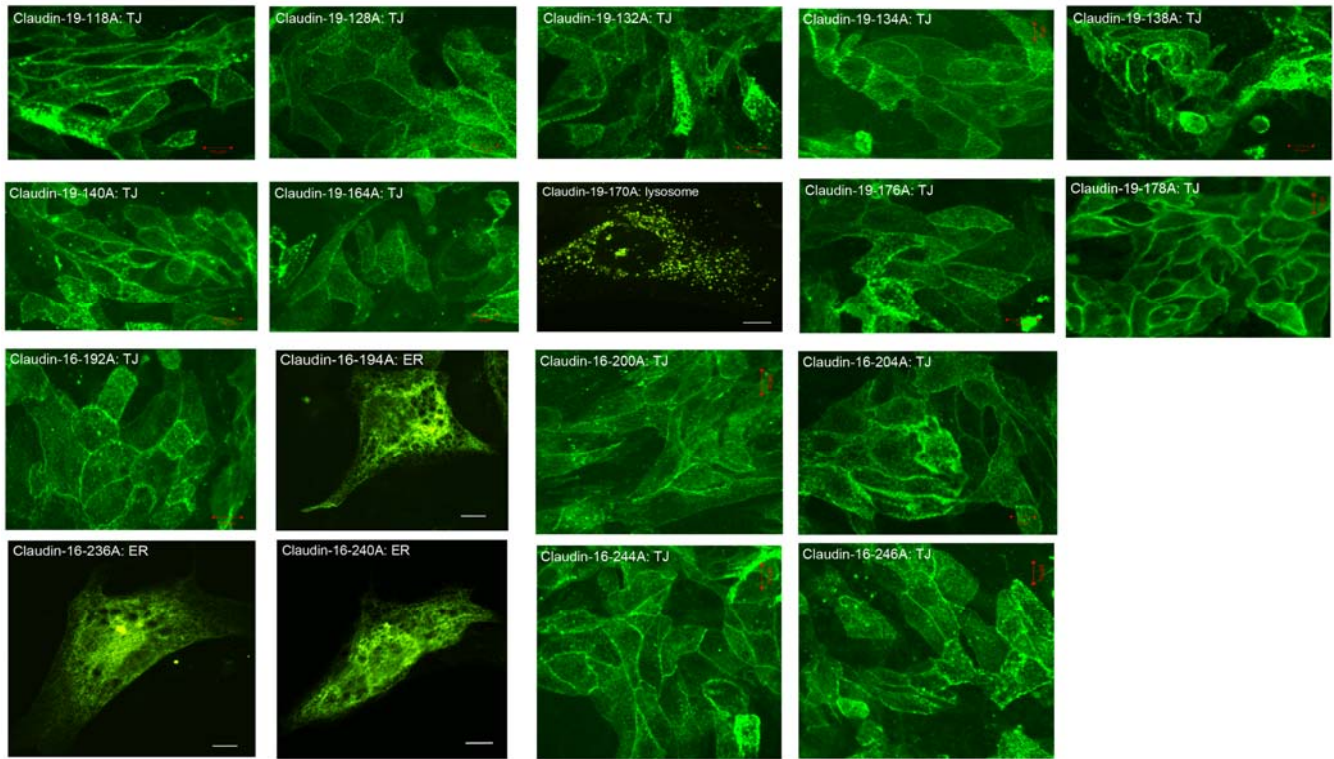
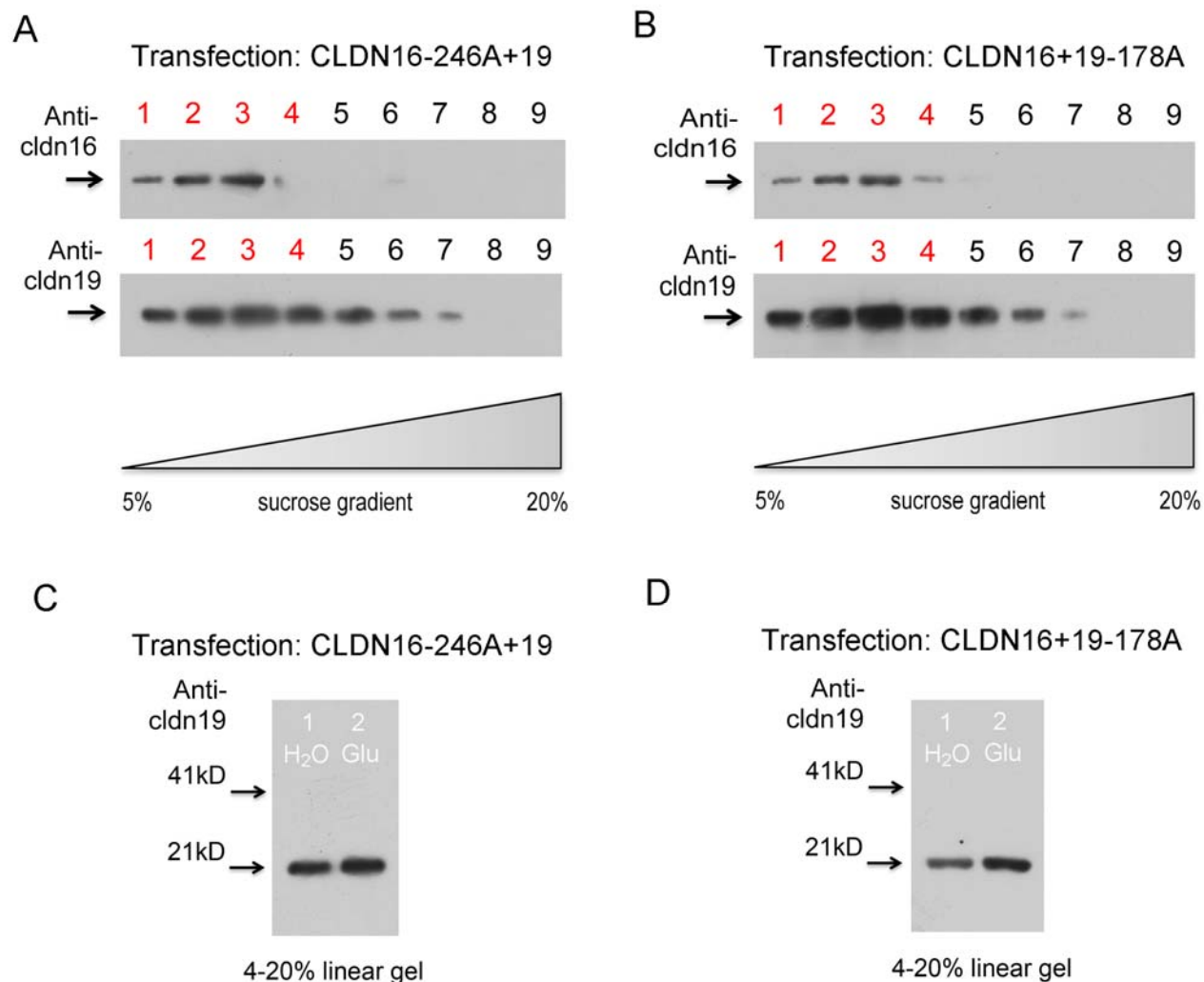


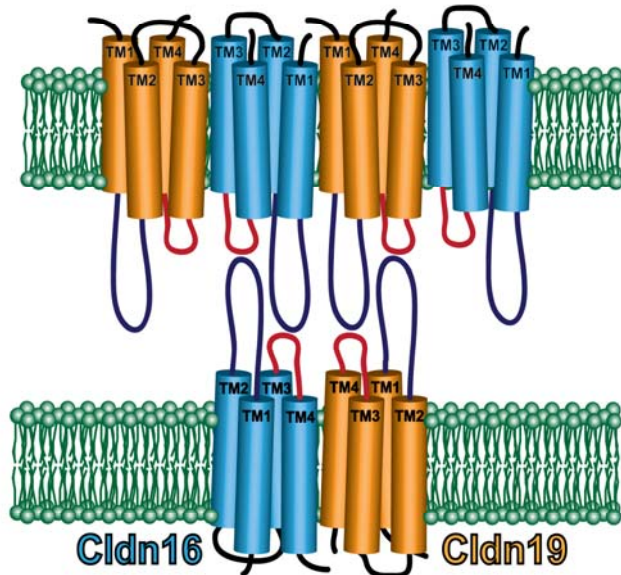
Figure S4. Effect of alanine insertion mutations on claudin localization. Confocal microscopy showed the subcellular localization of claudin-16 and -19 loss-of-interaction mutations. ER: endoplasmic reticulum; TJ: tight junction. Bar: 10 $\mu$ m.



**Figure S5.** Mutational effects on claudin-16 and -19 assembly in HEK293 cells. (A-B) Triton soluble cell lysate from doubly infected cells expressing cldn16-246A mutant with wildtype cldn19 (A) or cldn19-178A mutant with wildtype cldn16 (B) were fractionated on 5-20% linear sucrose gradients and blotted with anti-claudin-16 or anti-claudin-19 antibody. (C-D) The fractionated cell lysates from A and B were pooled, cross-linked with glutaraldehyde, and subjected to linear SDS-PAGE gel electrophoresis to determine the molecular weight of claudin oligomer and monomer.



A



B

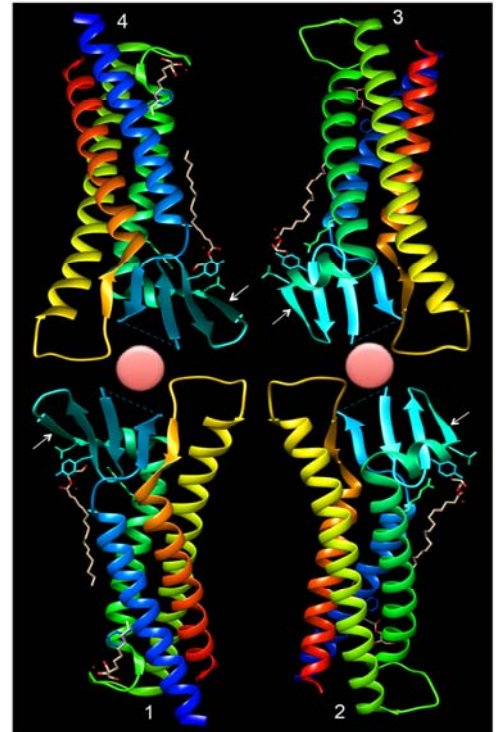


**Figure S6.** Claudin polymerization model in tight junction. (A) Cartoon showing how *cis*- and *trans*-interaction between claudin-16 and -19 polymerize them into tight junction strand. (B) Claudin interaction model based upon the 3D structure of claudin-15 to illustrate the ion permeation pore. Arrows indicate the 4<sup>th</sup>  $\beta$ -sheet of ECL1 where the charged residues contribute to the electrostatic field. Permeation ions are shown in red dot.

Table S1. Paracellular ion conductance in LLC-PK1 cells expressing claudin-19 and its loss-of-interaction mutants.

Construct	Position of mutation	TER ( $\Omega \cdot \text{cm}^2$ )	Dilution potential (mV)	$P_{\text{Na}}/P_{\text{Cl}}$	$P_{\text{Na}}$ ( $10^{-6} \text{ cm/s}$ )	$P_{\text{Cl}}$ ( $10^{-6} \text{ cm/s}$ )	Localization
vector	–	66.3 $\pm$ 0.7	–8.57 $\pm$ 0.07	0.272 $\pm$ 0.003	5.922 $\pm$ 0.105	21.750 $\pm$ 0.197	–
CLDN19-WT	–	136.3 $\pm$ 5.2	–0.57 $\pm$ 0.03	0.926 $\pm$ 0.004	6.493 $\pm$ 0.248	7.009 $\pm$ 0.265	TJ
CLDN19-118A	3rd TM	180.3 $\pm$ 1.5	–2.20 $\pm$ 0.12	0.742 $\pm$ 0.012	4.336 $\pm$ 0.066	5.843 $\pm$ 0.040	TJ
CLDN19-128A	3rd TM	143.0 $\pm$ 3.5	–0.97 $\pm$ 0.15	0.878 $\pm$ 0.017	6.009 $\pm$ 0.200	6.841 $\pm$ 0.117	TJ
CLDN19-132A	3rd TM	83.7 $\pm$ 3.0	–3.73 $\pm$ 0.07	0.599 $\pm$ 0.006	8.232 $\pm$ 0.266	13.760 $\pm$ 0.535	TJ
CLDN19-134A	3rd TM	138.7 $\pm$ 14.85	–0.37 $\pm$ 0.09	0.952 $\pm$ 0.011	6.596 $\pm$ 0.665	6.924 $\pm$ 0.664	TJ
CLDN19-138A	3rd TM	73.0 $\pm$ 2.0	–5.57 $\pm$ 0.03	0.456 $\pm$ 0.002	7.883 $\pm$ 0.183	17.293 $\pm$ 0.487	TJ
CLDN19-140A	3rd TM	155.0 $\pm$ 2.1	0.17 $\pm$ 0.03	1.023 $\pm$ 0.005	5.990 $\pm$ 0.092	5.856 $\pm$ 0.065	TJ

CLDN19-164A	4th TM	97.7±2.8	-2.70±0.06	0.692±0.006	7.699±0.198	11.130±0.368	TJ
CLDN19-170A	4th TM	68.3±0.9	-9.07±0.03	0.246±0.002	5.308±0.042	21.560±0.304	Lysosome
CLDN19-176A	4th TM	81.0±1.2	-3.97±0.03	0.579±0.003	8.311±0.141	14.357±0.182	TJ
CLDN19-178A	4th TM	154.3±3.4	-1.90±0.10	0.773±0.011	5.189±0.106	6.714±0.162	TJ
CLDN19-WT+CLDN16-WT	-	63.7±2.2	8.40±0.20	3.566±0.141	22.540±0.571	6.353±0.393	CLDN19 : TJ
CLDN19-118A+CLDN16-WT	CLDN19: 3rd TM	212.7±1.2	-0.03±0.03	0.996±0.004	4.306±0.034	4.325±0.015	CLDN19 : TJ
CLDN19-128A+CLDN16-WT	CLDN19: 3rd TM	170.7±5.8	3.80±0.06	1.687±0.014	6.766±0.213	4.013±0.159	CLDN19 : TJ
CLDN19-132A+CLDN16-WT	CLDN19: 3rd TM	101.0±1.0	0.83±0.12	1.119±0.018	9.600±0.166	8.576±0.022	CLDN19 : TJ
CLDN19-134A+CLDN16-WT	CLDN19: 3rd TM	176.3±1.5	1.93±0.03	1.300±0.006	5.883±0.038	4.527±0.048	CLDN19 : TJ
CLDN19-138A+CLDN16-WT	CLDN19: 3rd TM	88.3±1.5	0.13±0.07	1.018±0.009	10.487±0.136	10.303±0.208	CLDN19 : TJ
CLDN19-140A+CLDN16-WT	CLDN19: 3rd TM	202.7±1.2	2.93±0.03	1.492±0.007	5.423±0.040	3.634±0.016	CLDN19 : TJ
CLDN19-164A+CLDN16-WT	CLDN19: 4th TM	78.0±1.0	3.47±0.09	1.609±0.020	14.513±0.125	9.025±0.185	CLDN19 : TJ
CLDN19-176A+CLDN16-WT	CLDN19: 4th TM	108.3±1.5	-2.60±0.17	0.702±0.017	6.991±0.162	9.960±0.129	CLDN19 : TJ
CLDN19-178A+CLDN16-WT	CLDN19: 4th TM	194.7±3.0	0.27±0.15	1.037±0.020	4.802±0.109	4.631±0.056	CLDN19 : TJ



Table S2. Paracellular ion conductance in LLC-PK1 cells expressing claudin-16 and its loss-of-interaction mutants.

Construct	Position of mutation	TER ( $\Omega \cdot \text{cm}^2$ )	Dilution potential (mV)	$P_{\text{Na}}/P_{\text{Cl}}$	$P_{\text{Na}}$ ( $10^{-6} \text{ cm/s}$ )	$P_{\text{Cl}}$ ( $10^{-6} \text{ cm/s}$ )	Localization
vector	–	66.3±0.7	–8.57±0.07	0.272±0.003	5.922±0.105	21.750±0.197	–
CLDN16-WT	–	40.7±2.7	2.67±0.09	1.438±0.018	26.867±1.843	18.657±1.064	TJ
CLDN16-192A	3rd TM	49.0±2.5	–4.53±0.12	0.533±0.009	13.073±0.511	24.573±1.337	TJ
CLDN16-194A	3rd TM	65.3±1.8	–9.37±0.03	0.231±0.002	5.283±0.141	22.853±0.636	ER
CLDN16-200A	3rd TM	53.3±3.2	–6.83±0.24	0.372±0.015	9.407±0.706	25.270±1.555	TJ
CLDN16-204A	3rd TM	52.7±2.4	–2.00±0.10	0.763±0.010	15.133±0.598	19.867±1.061	TJ
CLDN16-236A	4th TM	67.3±0.3	–8.73±0.09	0.263±0.005	5.684±0.105	21.573±0.041	ER
CLDN16-240A	4th TM	72.7±1.7	–9.43±0.15	0.228±0.007	4.693±0.152	20.593±0.492	ER
CLDN16-244A	4th TM	57.7±2.2	–5.17±0.03	0.485±0.002	10.420±0.405	21.493±0.766	TJ
CLDN16-246A	4th TM	69.0±0.6	–6.10±0.06	0.419±0.004	7.857±0.015	18.747±0.208	TJ
CLDN19-WT+CLDN16-WT	–	63.7±2.2	8.40±0.20	3.566±0.141	22.540±0.571	6.353±0.393	CLDN16: TJ
CLDN19-WT+CLDN16-192A	CLDN16: 3rd TM	201.3±3.5	0.73±0.12	1.104±0.018	4.786±0.068	4.336±0.102	CLDN16: TJ
CLDN19-WT+CLDN16-200A	CLDN16: 3rd TM	199.7±3.2	–1.03±0.09	0.870±0.010	4.279±0.095	4.918±0.052	CLDN16: TJ
CLDN19-WT+CLDN16-204A	CLDN16: 3rd TM	195.7±1.5	2.00±0.06	1.312±0.010	5.323±0.058	4.058±0.012	CLDN16: TJ
CLDN19-WT+CLDN16-244A	CLDN16: 4th TM	160.3±10.3	0.17±0.15	1.023±0.020	5.846±0.450	5.702±0.338	CLDN16: TJ
CLDN19-WT+CLDN16-246A	CLDN16: 4th TM	178.7±2.4	1.03±0.20	1.151±0.032	5.496±0.085	4.781±0.109	CLDN16: TJ